© 2024. Published by The Company of Biologists Ltd | Journal of Experimental Biology (2024) 227, jeb247829. doi:10.1242/jeb.247829

RESEARCH ARTICLE

Body length determines flow refuging for rainbow trout (*Oncorhynchus mykiss*) behind wing dams

Terry R. Dial[1,2,*], Laura A. Collins[1], James C. Liao[3] and Bret W. Tobalske[1]

ABSTRACT

Complex hydrodynamics abound in natural streams, yet the selective pressures these impose upon different size classes of fish are not well understood. Attached vortices are produced by relatively large objects that block freestream flow, which fish routinely utilize for flow refuging. To test how flow refuging and the potential harvesting of energy (as seen in Kármán gaiting) vary across size classes in rainbow trout (*Oncorhynchus mykiss*; fingerling, 8 cm; parr, 14 cm; adult, 22 cm; n=4 per size class), we used a water flume (4100 l; freestream flow at 65 cm s^{-1}) and created vortices using 45 deg wing dams of varying size (small, 15 cm; medium, 31 cm; large, 48 cm). We monitored microhabitat selection and swimming kinematics of individual trout and measured the flow field in the wake of wing dams using time-resolved particle image velocimetry (PIV). Trout of each size class preferentially swam in vortices rather than the freestream, but the capacity to flow refuge varied according to the ratio of vortex width to fish length (W_V:L_F). Consistent refuging behavior was exhibited when W_V:L_F≥1.5. All size classes exhibited increased wavelength and Strouhal number and decreased tailbeat frequency within vortices compared with freestream, suggesting that swimming in vortices requires less power output. In 17% of the trials, fish preferentially swam in a manner that suggests energy harvesting from the shear layer. Our results can inform efforts toward riparian restoration and fishway design to improve salmonid conservation.

KEY WORDS: Wing dam, Vortex, Swimming, Kinematics, Particle image velocimetry

INTRODUCTION

Natural streams and rivers are characterized by complex flow patterns induced by substrates and barriers including rocks and logs (Liao, 2007; Cote and Webb, 2015). Fish living in moving water have the capacity to select microhabitats that are energetically favorable using their lateral line system and vision (Liao, 2006). Field studies have confirmed that chosen flow conditions and substrates vary with size class during ontogeny (Baltz et al., 1991; Ayllón et al., 2010), and the large size of adult fish may preclude their access to certain habitats (Rosenfeld and Boss, 2001). Along with flow conditions, other selective pressures influence selection of microhabitats, including competition (Lohr and West, 1992), predation risk and rate of food acquisition (Rosenfeld and Boss, 2001; Kalb et al., 2018; Johansen et al., 2020).

Fish are known to take advantage of flow near structures to reduce the energetic cost of being in moving water (Liao, 2007; Cook and Coughlin, 2010; Taguchi and Liao, 2011; Currier et al., 2021). This may be in the form of flow refuging in the lower velocity wake behind a bluff body, but also via lateral entrainment, positioning upstream in the bow wake region, or via vortex capture (Liao and Cotel, 2013; Pentaluna et al., 2021; Harvey et al., 2022). For example, trout in a water flume adopt the Kármán gait to harvest energy from alternating vortices of a von Kármán street (Liao et al., 2003a). These vortices are consistently shed in the wake of a D-cylinder and reduce the recruitment of muscle and oxygen needed by a fish relative to that required to swim in the freestream. Fish slalom between the alternating vortices, harvesting kinetic energy in the flow produced in the Kármán street.

Kármán gaiting is a well-characterized swimming behavior in flow, having benefited from kinematic, electromyography, respirometry and hydrodynamic analysis (Liao et al., 2003a,b; Liao, 2004; Beal et al., 2006; Taguchi and Liao, 2011). Kármán gaiting in the well-known flow behind a bluff body (i.e. Kármán street) can provide initial insight into how trout swim in other types of unsteady flows. For example, the ability to Kármán gait requires the body length to be a certain size in relation to the diameter of the cylinder that is producing the Kármán street (Akanyeti and Liao, 2013). Fish Kármán gait when the ratio of cylinder diameter to fish length falls between 1:2 and 1:4. As this ratio increases, body wavelength covaries with the wavelength of the shed vortices in the Kármán street (Akanyeti and Liao, 2013). As the diameter of vortices in the wake is similar to cylinder diameter, fish harvest energy from a Kármán street when vortices are 25–50% of their length. Among size classes of fish, tailbeat frequency varies with shedding frequency of the vortices rather than as a function of body length. In light of previous studies of fish holding station in unsteady flows, we asked whether that was a similar size relationship in the more relevant ecological context of wing dams, which are prevalent in streams and rivers worldwide.

In contrast with saving energy in low velocity flow or in predictable vortical flows, fish avoid fully turbulent flows that are characterized by high turbulent kinetic energy (TKE; Kerr et al., 2016; Sirajee, 2023) and acceleration (Enders et al., 2009). Turbulence, with random fluctuations in three-dimensional velocity, destabilize fish and incur additional energy costs (Enders et al., 2003). Such effects due to perturbation are predicted to vary with vortex size relative to fish size and are particularly destabilizing when the size of a vortex is approximately the same as body length (Cote and Webb, 2015). Another goal of our study was to provide a novel test for a relationship between vortex and fish sizes.

The majority of work examining the microhabitat selection of fish swimming in unsteady flows has been performed in the wake of D-cylinders (Liao, 2007). Here, we sought to expand our understanding of how fish interact with structures found commonly

[1]Field Research Station at Fort Missoula, Division of Biological Sciences, University of Montana, Missoula, MT 59812, USA. [2]Utah State University Moab, Moab, UT 84532, USA. [3]Department of Biology, The Whitney Laboratory for Marine Bioscience, University of Florida, St Augustine, FL 32080, USA.

*Author for correspondence (terry.dial@usu.edu)

T.R.D., 0000-0002-4737-1875; J.C.L., 0000-0003-0181-6995; B.W.T., 0000-0002-5739-6099

Received 4 April 2024; Accepted 7 July 2024

in real-world environments. Boulders deflect the flow of moving water and produce a recirculating vortex on the lee side of the boulder (Bouckaert and Davis, 1998). We chose to use wing dams as analogous structures to boulders to simplify and standardize the geometry of the obstructions, as well as utilize a common fish ladder baffle design. We hypothesized that fish are attracted to flow regimes that display predictable flow. We also hypothesized that fish avoid strong turbulence (Liao, 2007) and well as vortices with dimensions approaching their body length (Cote and Webb, 2015).

Along current-swept habitats, salmonid fishes (Family Salmonidae) are celebrated for their migratory (both local and sea-run, anadromous) prowess. But range contractions and declines in abundance indicate these species are threatened (Penaluna et al., 2016). Current management efforts for maintaining salmonid populations focus on habitat conservation, longitudinal connectivity of populations and life history diversity (Williams et al., 2011). Physical impediments, such as large water impoundments and narrowing and simplifying river channels, restrict returns, often at specific stages of life history. To maximize upstream return numbers around impoundments, vertical slot ladders, composed of alternating wing dams, are designed with velocity, TKE and flow patterns (vorticity) in mind (Hameed and Hilo, 2021). Fishery managers have constructed wing dams composed of boulders to improve habitat for trout in streams (Shuler et al., 1994). Vertical-slot fishways are effective in restoring passage in inland streams (Hodge et al., 2017). Passage success of species such as brown trout (*Salmo trutta*) and rainbow trout (*Oncorhynchus mykiss*) depends on the impeding structure (baffle, ramp, weir; Forty et al., 2016), and it is recommended that the designs of such passages consider different size classes of fish (Forty et al., 2016).

Trout exhibit broad sympatry of size classes throughout their life history (McPhee et al., 2014) and body size varies over an order of magnitude throughout ontogeny (Jonsson and Jonsson, 1998), which dictates resource use and predation risk (Werner and Gilliam, 1984; Rosenfeld and Boss, 2001). Previous studies have shown predictable variation in micro-habitat selection across ontogeny in trout (Rosenfeld and Boss, 2001; Ayllón et al., 2010). Juvenile brown trout prefer to swim behind wing dams artificially constructed of multiple boulders in natural streams, particularly when flow rates are high (Shuler et al., 1994).

To understand the interaction more fully between fish size and common structures impeding flow in streams and rivers, herein we provide a novel test of the behavior and kinematics of rainbow trout of different size classes in relation to flow dynamics as the fish were swimming in the vicinity of wing dams that varied in size. We tested whether kinematics and microhabitat selection varied among size classes and dam sizes. We examined trout orientation, position and midline kinematics to test for (i) preference for vortices and (ii) position in the shear layer formed between the freestream and vortex in a manner that might reduce the energetic costs of the overall swimming budget.

MATERIALS AND METHODS

Trout collection and husbandry

Rainbow trout, *Oncorhynchus mykiss* (Walbaum 1792), were obtained from Harriman hatchery in St Ignatius, MT, USA, and were housed at the Field Research Station at Fort Missoula under University of Montana IACUC Animal Use Protocol 007-20BTDBS-033020 and a transport permit from Montana Fish Wildlife and Parks (13015-8-0320-3). Caution is always warranted when interpreting the ecological or evolutionary significance of experiments using hatchery fish. Although we did not detect gross morphological and physiological differences from wild populations, they are known to exist (e.g. Gale et al., 2004). Four individuals in each of three size classes of fish were used in this study: fingerlings (mean±s.e.m. 8.6±0.7 cm standard length, SL), parr (14.3±0.2 cm SL) and adults (22.6±1.2 cm SL) and housed in 189 l tanks with adults separated from younger fish. The fish were fed twice daily for a duration of 5 min on pellet food (fingerlings and parr: Aquamax Grower 400; adults: Aquamax Sport Fish 500; Purina Animal Nutrition LLC., Gray Summit, MO, USA). The fish were maintained on a 12 h:12 h light:dark schedule.

Water temperature was set at 15°C and controlled using AquaEuroUSA MC 1/2HP chillers (AquaEuroUSA/Hamilton Technology, Los Angeles, CA, USA). We filtered the water using combinations of Fluval 307, 407 and FX6 filters (Fluval Aquatics USA, Rolf C. Hagen, Inc., Mansfield, MA, USA). Water was driven through the chillers and filters using BlueLine 10 HD (BlueLine Aqua, Champion Lighting and Supply Co., Ltd, Ambler, PA, USA) and ActiveAQUA AAPW250 (Active Aqua, Petaluma, CA, USA) pumps. To oxygenate the water, we used Imagitarium air pumps (International Pet Supplies and Distribution, Inc., San Diego, CA, USA) and a custom-made sprinkler system.

The water in the tanks was municipal (tap) water treated with Kordon Amquel Plus Water Conditioner that eliminates nitrite, nitrate, ammonia, chloramines and chlorine in fresh water and Kordon NovAqua+ Plus Water Conditioner that detoxifies tap water, removes chlorine and heavy metals and balances pH. We monitored and modified water quality daily using an API Freshwater Aquarium Master Test Kit (API Fishcare, Chalfont, PA, USA) that tests for pH, high range pH ammonia, nitrate and water hardness. We modified pH using API pH Up or API pH Down solution as needed to maintain pH at 7.0 and, if necessary, given the guidelines in the Master Test Kit, removed ammonia, nitrates or water hardness by treating the water using Amquel Plus and NovAqua+. We conducted 20% water change in the tanks 3 times weekly, siphoning water from the bottom of the tanks.

Experimental flume

Our water flume (Fig. 1) was custom fabricated using aluminium (3.2 mm thick) and contained 4100 l of water monitored and conditioned as described above for the holding tanks. We maintained the temperature at 15°C using an AquaEuroUSA MC-1HP chiller and a Blue Line 4UXHD pump. To drive water flow, we used two Minn Kota Endura MAX 55-36 transom-mount trolling motors (Johnson Outdoors, Inc., Racine, WI, USA) set to 75% power. This gave an average freestream flow velocity in the test section of 65 cm s^{-1} (Fig. 2A). The test section of the flume measured 100 cm×160 cm×40 cm (width×length×height; Fig. 1). A transparent Plexiglas window (50 cm×25 cm, 6.4 mm thick) allowed for lateral views into the test section, and we projected laser light through this window for particle image velocimetry (PIV; see below). Upstream of the working section, water moved through a 10.2 cm deep aluminum (ACG) honeycomb panel (Hexcel Corp., Stamford, CT, USA), with >95% open area and a cell diameter of 9.5 mm.

Individual fish were placed in the test section of the flume with one of three different experimental wing dam treatments: small (15.2 cm), medium (30.5 cm) and large (48.2 cm). The wing dams were constructed of clear acrylic (6.4 mm thick) and presented at a 45 deg angle to the oncoming flow so that the trailing edge was downstream. The lateral distances the dams projected into the oncoming flow (i.e. dam widths) were 10.7 cm, 21.6 cm and 34.1 cm for the small, medium and large dams, respectively.

Journal of Experimental Biology (2024) 227, jeb247829. doi:10.1242/jeb.247829

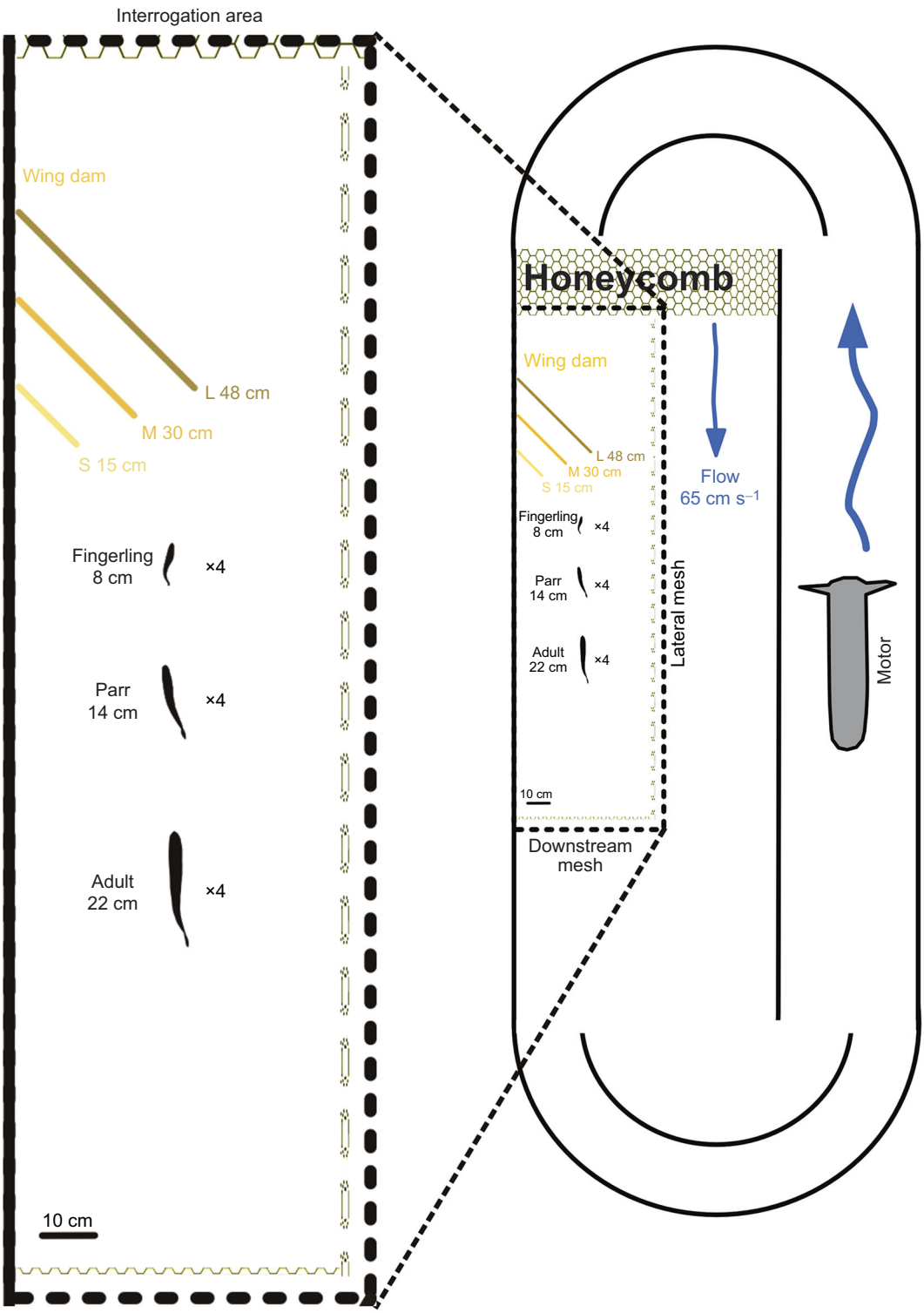

Fig. 1. Experimental design. We used a water flume with flow velocity set at 65 cm s^{-1} and used video (10 Hz for microhabitat selection; 250 Hz for undulatory kinematics) to study swimming in three size classes of rainbow trout (*Oncorhynchus mykiss*): fingerling (8 cm), parr (14 cm) and adult (22 cm) (*n*=4 per size class). The three different experimental wing dam treatments are indicated (small, 15 cm; medium, 30 cm; and large, 48 cm).

PIV

The flow field of the test section of the flume was measured using time-resolved PIV. We illuminated the flow field using an Nd:YLF dual cavity, dual head, 30 mJ/pulse Nd:YLF laser (Model MD30-527DH, Photonics Industries International, Inc. Ronkonkoma, NY, USA) with a LaVision articulating light delivery arm (LaVision GmbH, Göttingen, Germany). We seeded the water using hollow glass spheres 8–12 µm in diameter (TSI Incorporated, Shoreview, MN, USA) and had interrogation window sizes of 50 cm×50 cm. We recorded video (100 Hz, duration 5 s) in double-frame exposure mode (ΔT=4.9975 ms) using a Nova S6 camera (Photron, San Diego, CA, USA) controlled using DaVis 10.2.0 software and a PTUX

Journal of Experimental Biology (2024) 227, jeb247829. doi:10.1242/jeb.247829

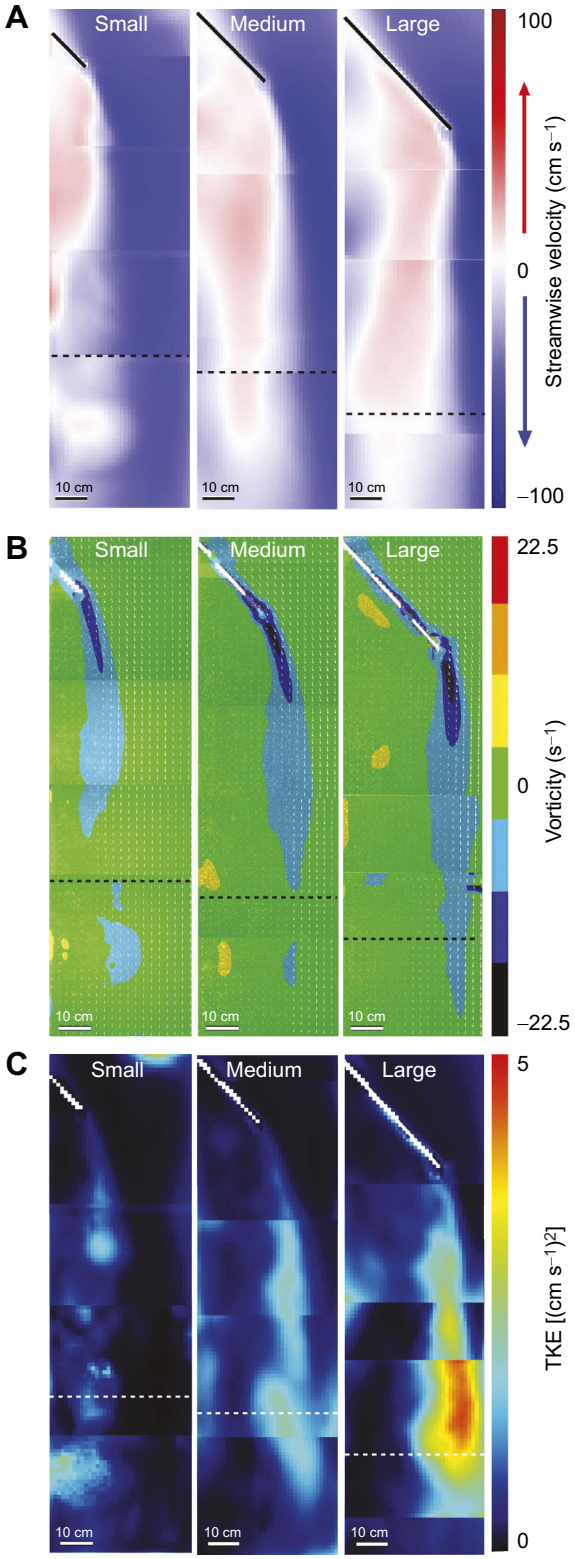

Fig. 2. Composite images of patterns of water flow induced by the three sizes of wing dam as measured using time-resolved particle image velocimetry (PIV). (A) Streamwise velocity. (B) Vorticity. (C) Turbulent kinetic energy. Horizontal dashed lines indicate the downstream limit of the interrogation area for sampling of swimming behavior.

programmable timing unit. Our PIV analysis used DaVis for cross-correlation of image pairs and multi-pass processing with initial interrogation window size at 64 pixels×64 pixels ending with 48 pixels×48 pixels with 50% overlap. Maximum expected pixel displacement was 12 pixels; we used post-processing with an allowed vector range of 0–20 pixels, deleting vectors if correlation <0.5, 3× median filtering and filing of empty spaces using interpolation. We computed average flow characteristics from 500 PIV fields and herein report streamwise velocity (cm s^{-1}), vorticity (s^{-1}) and turbulent kinetic energy [(cm s^{-1})^2].

We reconstructed the flow field of the test section of the flume in the vicinity and downstream of the wing dams by manually compiling our 50 cm×50 cm PIV images into composite (44 cm×136 cm, width×length) images of velocity, vorticity and turbulent kinetic energy. This was facilitated using images of calibration rulers with reference to the trailing edge of the wing dams.

Behavioral data

Each trout was allowed to acclimate in the flume for 30 min prior to each swimming trial. Each trial had a different size of dam (small, medium or large) placed in the test section of the flume. The flume was then set at 75% power setting and the fish was allowed to swim within a 160×60 cm area bounded by the wall of the flume and barriers of galvanized steel mesh (0.8 mm wire diameter, 12 mm diameter square openings; Fig. 1). We used top-down digital videography (Photron FASTCAM NOVA S6 camera), set to 10 Hz record rate (shutter speed 5000 s^{-1}), to capture swimming behavior. We used recordings of a 30.5 cm wand to calibrate the videos to metric coordinates using the app DLTdv8 (Hedrick, 2008) in MATLAB (R2021a, MathWorks, Natick, MA, USA). Our target sample time per fish was 10 min, but variation in the amount of time fish swam within the camera view of the test section resulted in an average sample time of 8.9±0.6 min with six of 36 trials (16%) including non-contiguous recordings. This behavioral dataset enabled us to measure each individual trout's preference on location (cross-stream and streamwise position, cm) and orientation (head oriented upstream versus downstream) in each flow environment.

We used DeepLabCut v2.2 (DLC, UPMWMATHIS Lab, Geneva, Switzerland; Mathis et al., 2018; Nath et al., 2019) to track the position and orientation of the head of each fish in our video recordings. We used a different training set for each size class, compiling all videos for all three dams (n=12 videos for each fish size), and a random subset of 20 frames, selected by DLC, from each of those 12 videos. We specified three anatomical landmarks: tip of snout, left eye and right eye. We then trained the DLC program on those three points for all 240 training set frames using the following parameters: resnet=50, display iterations=100, save iterations=1000 and max iterations=200,000, and 'filter predictions' was applied to the output files.

We used custom scripts in MATLAB to compute behavioral variables that describe the position and orientation of each fish collected in the behavior filming trial. We first eliminated rows from the output of DLC whenever a likelihood for any anatomical point was <0.95. To avoid biasing towards individuals with larger datasets, we down sampled using random elimination of data rows so that the number of video frames was equal among all individuals for a given size class and dam size. We referenced all metric positions (cm) relative to the trailing edge of a given wing dam. We calculated the position of the center of the fish's head as the mean among the snout and eye points. We measured fish orientation (upstream or downstream) by computing the angle between the cross-stream and a position vector from the center of its head to its snout. We used the 'hist3' function in MATLAB to generate bivariate histograms (surface plots) that summed all values for center of head within 5 cm×5 cm bins.

Journal of Experimental Biology (2024) 227, jeb247829. doi:10.1242/jeb.247829

Kinematics

To measure details of body motion, we recorded 250 Hz (shutter speed 5000 s^{-1}) video using the same Photron FASTCAM NOVA S6 camera as used in the behavioral sampling. We recorded swimming of individual fish within the test section in the vicinity of each dam size (small, medium and large) and within two different flow conditions (vortex and freestream). We used the custom script 'Clickdigfish_matlab2015a' (Liao et al., 2003b) in MATLAB to measure kinematic variables from one complete cycle of undulation per fish, dam size and flow condition. We measured tailbeat frequency (f, Hz), wavelength (cm) and amplitude (a, cm). We then computed Strouhal number (St):

$$St = \frac{fa}{|v|}, \quad (1)$$

where v is streamwise flow velocity (cm s^{-1}; with downstream considered negative).

To provide insight into how kinematics varied within a longer bout of swimming, we digitized one sequence of 3 s of swimming by an adult starting in the vortex of a large dam and exiting to the freestream. We digitized anatomical landmarks along the midline of the body using DLTdv8 in MATLAB.

Statistical analysis

Our experimental design involved repeated measures within individuals, so to test for significant differences among size classes, dam sizes and flow conditions, we used two-way mixed ANOVA in R (v4.2.2, http://www.R-project.org/) with functions 'anova test()' and 'get anova table' in the rstatix package. We used age (fingerling, parr and adult) as between-subject factors. Dam sizes (small, medium and large) were within-subject factors for behavioral variables: time oriented upstream (%), time in vortex (%), cross-stream position (cm) and streamwise position (cm). Flow conditions (freestream or vortex) were within-subject factors for kinematics variables: wavelength (cm), tailbeat amplitude (cm), tailbeat frequency (Hz) and Strouhal number (St). For kinematics variables in the two-way models, we first computed within-subject means within vortex or freestream among the three dam sizes. We report means±s.e.m.

RESULTS

PIV

The size of the wake increased with increasing dam size, but we observed generally similar flow patterns among dam sizes as represented by streamwise velocity, vorticity and TKE (Fig. 2). Each wing dam produced a vortex, or downstream recurrent flow structure, with streamwise flow velocities in the center of the vortex averaging 8.7, 7.9 and 6.8 cm s^{-1} for small, medium and large dams, respectively. Streamwise freestream velocity averaged −58, −59 and −68 cm s^{-1} for small, medium and large dams, respectively (negative values represent downstream flow). Peak values of ∼−100 cm s^{-1} were exhibited near the trailing edge of the wing dams facing toward the freestream. The distance before downstream reattachment of freestream flow to the lateral wall of the flume was positively correlated with wing dam size, and wake widths were slightly greater than dam widths. Using streamwise velocity (Fig. 2A) and the inflection of 0 cm s^{-1} at flow reversal to define the edges of the vortices, vortex sizes (length×width) were 84.1 cm×15.5 cm, 118.3 cm×25.5 cm and 121.3 cm×34.3 cm.

Negative vorticity (i.e. clockwise rotation as viewed from above) resulted from shear between the water immediately behind the dam and that in the freestream. This vorticity was attached to the trailing edge of each wing dam and the greatest magnitude (−22.5 s^{-1}) was exhibited in the near-wake of the trailing edge of the large dam (Fig. 2B). Smaller patches of lower positive vorticity (∼11 s^{-1} counter-clockwise) were produced within and downstream of the dams (Fig. 2B). The time-averaged vorticity in the shear layer was stable behind all three dams (Fig. 2B), but variation including shedding of vortices was apparent in instantaneous images of the wake (Fig. S1). Measuring wake dimensions using a negative vorticity threshold of −3 s^{-1} (13% of peak negative vorticity), the length×width was 87.3 cm×27.3 cm, 99.0 cm×41.3 cm and 131.6 cm×48.4 cm.

The magnitude and scale of TKE varied with dam size (Fig. 2C). TKE remained lower in magnitude in the wake of small and medium dams, reaching peak values of ∼2 (cm s^{-1})^2, whereas from 70–90 cm downstream of the edge of the large dam, TKE was over twice as large, reaching a peak value of 5 (cm s^{-1})^2.

Behavior

Individual fish varied in head orientation while in the wake of wing dams and exhibited preferences for specific locations (Fig. S2). For example, a parr swimming downstream from the small dam swam only briefly within the vortex of the dam, and ranged cross-stream to ∼45 cm into the freestream (Fig. S2A), and its peak frequency of location was 70 cm downstream and 30 cm into the freestream (Fig. S2C). The overall tendency of the parr was to orient upstream, yet it was oriented downstream as it turned from the freestream into the shear layer trailing from the edge of the wing dam and circled back to the freestream (Fig. S2A). When swimming in the vortex behind the medium dam, this fish oriented itself in the direction of oncoming flow, so was positioned downstream in the global frame of reference. In contrast, this fish faced upstream while in the freestream flow offboard from the wing dam (Fig. S2B). This individual preferentially swam 40 cm downstream and 15 cm inboard from the edge of the wing dam (Fig. S2D).

Fish preferred to swim in the vortex of a dam if the dam was large enough to permit refuging behavior (Fig. 3). Parr and especially adults seldom swam in the vortex of the small dam. Unique patterns were apparent for each combination of fish and dam size. For example, fingerlings spent most of their time within 20 cm downstream of the small dam but were spread further downstream in the vortices behind the medium and large dams (Fig. 3). Parr spent most of their time downstream of the small and medium dams and positioned themselves immediately behind the large dam (Fig. 3). Parr, particularly one individual among the four, also exhibited a unique tendency to swim in the freestream flow located upstream of the dam. In the presence of small and medium dams, adults spent more time in the freestream than smaller trout but spent a high frequency of time positioning themselves immediately behind the large dam.

Fish orientation was a function of body and dam size and likely a product of local flow regime depending on the position of the fish in the flume. The percentage of time spent swimming oriented upstream varied significantly with dam size (ANOVA: d.f., 2,18; P=0.00075). In the presence of the small dam, fingerlings were mainly oriented forward (i.e. towards the top of the flume; this does not indicate whether the fish was swimming into or out of the local flow; Fig. 4A). As dam size increased, fingerlings increased the amount of time oriented downstream – up to 75% of total time pointed downstream with the large dam (Fig. 4A). Parr spent most of their time swimming forward in the small dam, but then spent most of their time oriented downstream in the wake of the medium and large dams. This trend was similar in adults, except that for medium and large dams, adults split their time evenly between being oriented upstream and downstream (Fig. 4).

Journal of Experimental Biology (2024) 227, jeb247829. doi:10.1242/jeb.247829

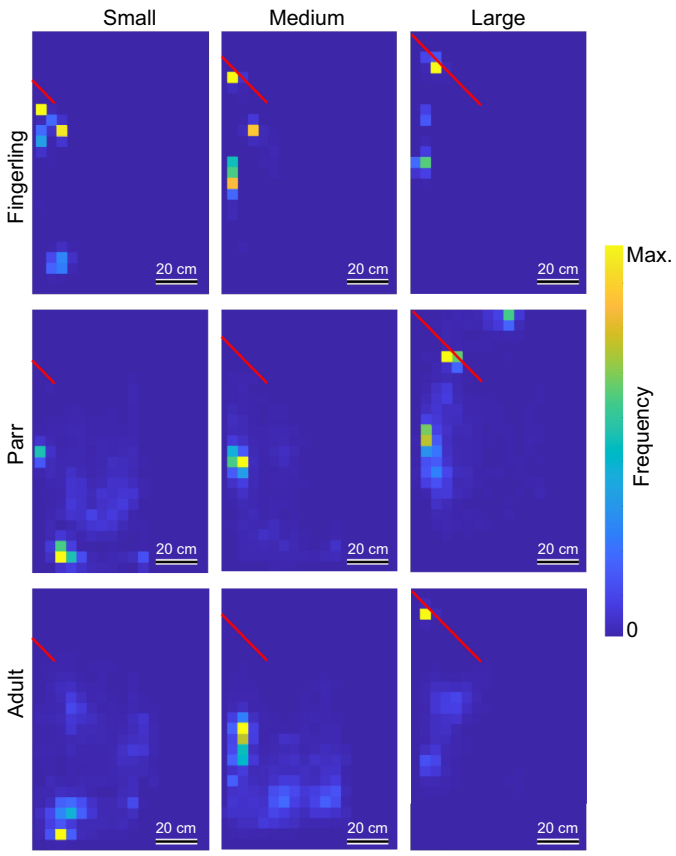

Fig. 3. Frequency distributions of microhabitat selection in the three size classes of rainbow trout swimming in the vicinity of the three different sizes of wing dam. *n*=4 fish per class: fingerling, parr and adult. Red lines represent wing dams (small, medium and large). Total count for each combination of size class and dam size averaged 14,513 (range 9304–20,212), with each count divided equally among four fish per size class. Cell sizes within the grids are 5 cm×5 cm.

The amount of time spent in the downstream vortex created by each wing dam changed significantly with size class (ANOVA: d.f., 2,9; P=0.0028 for size class and d.f.=2,18, P=0.000006 for dam size). For the small dam, fingerlings spent 3–4 times longer within the vortex compared with their larger counterparts (Fig. 4B). Behind the medium dam, vortex holding was an inverse function of fish size, where fingerlings spend the most time, and adults the least (Fig. 4B). All fish were able, and preferred, to spend nearly 100% of their time in the vortex behind the large dam (Fig. 4B).

Cross-stream position varied significantly with size class (ANOVA: d.f. 2,9; P=0.01) and dam size (ANOVA: d.f., 2,18; P=0.000001; Fig. 4C,D). Smaller fish were able to position themselves further into the vortex for any given dam size; and for the small dam condition, parr and adults were restricted to swimming in the freestream flow. Streamwise positioning behavior showed that smaller fish held closer to the dam and that fish of any size got closer to the dam as dam size increased. The mean streamwise position varied significantly with size class (ANOVA: d.f. 2,9; P=0.018) and dam size (ANOVA: d.f. 2,18; P=0.005).

None of the interactions between the effects of size class and dam size were statistically significant for time oriented upstream, time in vortex, cross-stream position or streamwise position (ANOVA: d.f. 4,18; all P>0.29).

In two conditions (17% of all possible combinations of size class and dam size), fish exhibited swimming locations and orientation that may have offered opportunities to harvest energy from the shear layer between the vortex and the freestream. Fingerlings swimming behind small dams and adults swimming behind medium dams exhibited cross-stream positions on the inside edge and centered on the edge of the dam, respectively (Fig. 4C). During these trials, fingerlings oriented upstream 80% of the time compared to 58% for adults.

Kinematics

Swimming kinematics varied as a function of fish size and flow regime (vortex versus freestream). Individual fish searched the experimental test section, crossing in and out of the shear layer between the vortex and the freestream (Figs S2, S3). Transitioning from the vortex (red background in Fig. S3A) to the freestream (blue background in Fig. S3A) changed the swimming kinematics observed in an individual fish (Fig. S3B). The fish turned upstream when exiting the wake of the dams so that their heads were oriented into the flow when entering the freestream (Fig. S3A).

Relative freestream swimming velocity ranged from 4 body lengths (BL) s^{-1} in adults to 12 BL s^{-1} in fingerlings; requiring relatively short undulation wavelengths and high tailbeat frequency to station hold (Fig. 5). Within the vortex, each size class exhibited longer wavelengths, lower tailbeat frequencies and higher Strouhal numbers than when swimming in the freestream (Fig. 5). Local flow condition (vortex versus freestream) had significant effects upon mean tailbeat frequency (ANOVA, d.f. 1,9; P=0.000001), wavelength (ANOVA, d.f. 1,9; P=0.01) and *St* number (ANOVA: d.f. 1,9; P=0.000006). Size had significant effects on mean tailbeat frequency (ANOVA: d.f, 2,9; P=0.000003) and *St* number (ANOVA: d.f. 2,9; P=0.00016). There was a significant interaction effect between size class and flow condition for tailbeat frequency (ANOVA: d.f. 2,9; P=0.0003) but not for mean wavelength and *St* number (both P>0.45). In both vortex and freestream swimming, *St* number declined with increasing body size. Parr and adults were able to achieve $0.2 \leq St \leq 0.4$ when swimming in the freestream, but fingerlings averaged a *St* number 0.8±0.2 (Fig. 5D). Tailbeat amplitude did not vary significantly with size class, dam size or an interaction between the two (all P>0.43). Expressed relative to body length, relative tailbeat amplitude declined with increasing body size, from 0.53 in fingerlings, to 0.32 in parr and 0.21 in adults (1/total length). Relative to body length, relative wavelength also decreased with increasing size from 0.25 in fingerlings, to 0.23 in parr and 0.19 in adults.

DISCUSSION

Size-selected refuging behavior

Our results revealed that all three size classes preferred to position themselves within a vortex, but their capacity to do so differed as a function of dam size. Cote and Webb (2015) recommended using a dimensionless ratio of vortex size to improve understanding of the propensity of a wake structure to destabilize a swimming fish. If we use streamwise velocity (Fig. 2A) to define wake size, we obtain vortex width to fish length (W_V:L_F) ratios that vary from 0.7 (adult with small dam) to 4.0 (fingerling with large dam). When W_V:$L_F \leq 1.1$, as was the case for parr and adults with small dams and adults with medium dams, refuging behavior was not exhibited or appeared to be constrained (Figs 3 and 4). Flow refuging was consistently performed when W_V:$L_F \geq 1.5$. Wake widths would be greater if defined using vorticity instead of streamwise velocity, so, defined using vorticity, the threshold above which all size classes of trout would regularly flow refuge would be W_V:$L_F \geq$ 2.1. Using either variable to define wake width, having a wake that is larger than body length seemed to best accommodate flow refuging. Vortices that have the greatest potential to perturb swimming are

Journal of Experimental Biology (2024) 227, jeb247829. doi:10.1242/jeb.247829

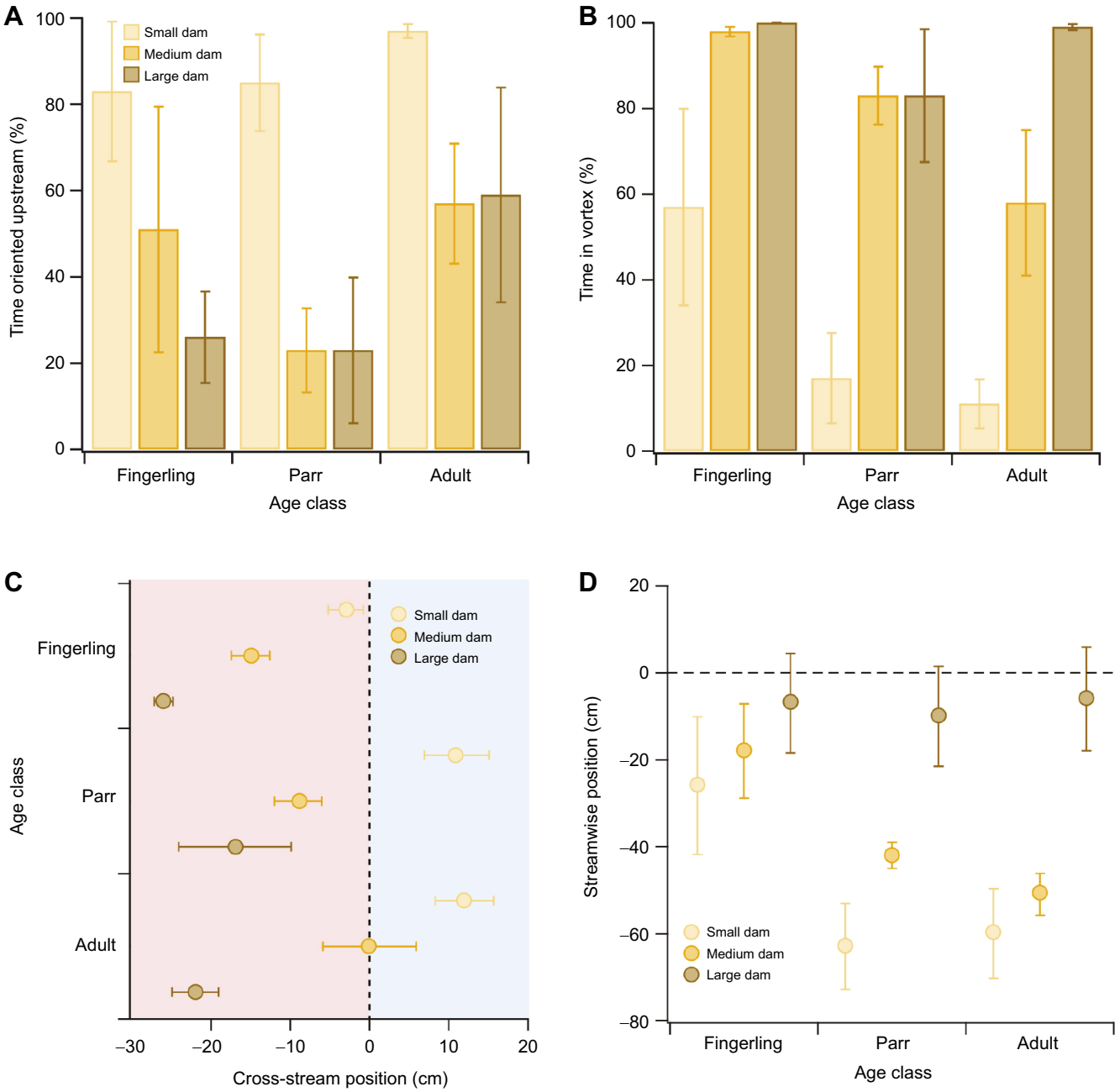

Fig. 4. Behavioral data for the three size classes of rainbow trout swimming in the vicinity of the three different sizes of wing dam. *n*=4 fish per class: fingerling, parr and adult. (A) Percentage of time spent oriented upstream. (B) Percentage of time spent in the vortex of the wing dam. (C) Cross-stream position relative to the tip of the wing dam; negative values (red) are in the vortex. (D) Streamwise position relative to the tip of the wing dam; negative values (below the dashed line) are downstream.

approximately of the same spatial scale as a characteristic length of an animal (Tritico and Cotel, 2010; Cote and Webb, 2015). Thus, we interpret that parr and adult trout avoided swimming in vortices of small dams to maintain their swimming stability.

Trout behavior varying according to W_V:L_F ratio may provide useful insight into micro-habitat preferences of different size classes of trout when interpreting ecological needs (Rosenfeld, 2003). For example, W_V:L_F ratio could be used to determine the size of boulders or other objects to be selected when creating refugia specifically for different size classes of trout in stream restoration (Shuler et al., 1994) or when building artificial passageways to help fish circumvent dams (Forty et al., 2016). Fisheries managers and others working in natural streams are not likely to have ready access to PIV or other methods for measuring wake dimensions, so the ratio of dam width to body length is a potentially useful substitute. Trout appeared to fully flow refuge when this ratio was greater than 1.2. However, one limitation of this alternative for making specific predictions of behavior is that the relationship between dam width and wake width was not linear. Dam width was 70%, 85% and 99% of wake width for small, medium and large dams, respectively.

Shared patterns of behavior among size classes

Changing dam size changed trout behavior and kinematics in a manner consistent with size-selected refuging. Across trout size

Journal of Experimental Biology (2024) 227, jeb247829. doi:10.1242/jeb.247829

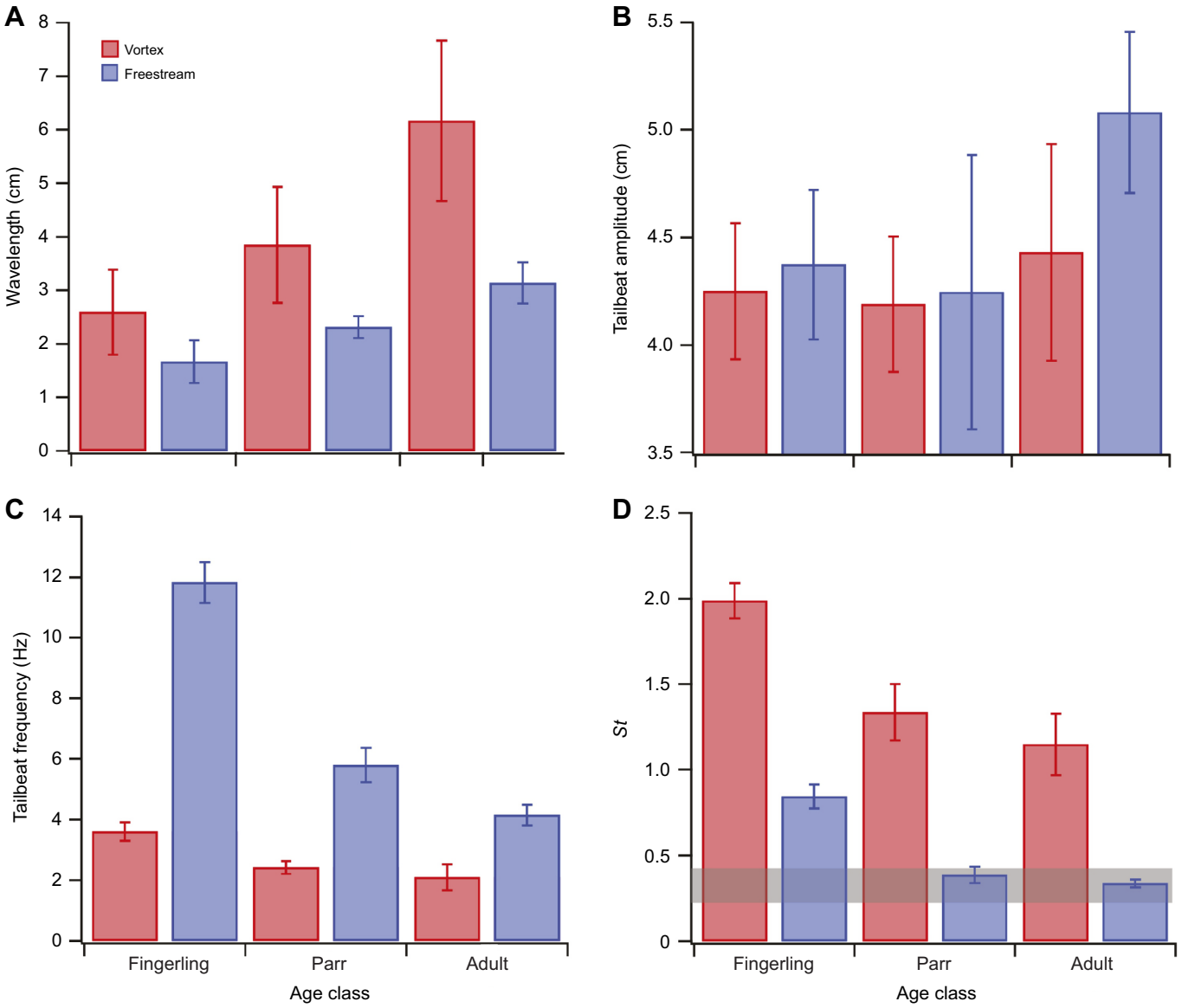

Fig. 5. Swimming kinematics in the three size classes of rainbow trout swimming in the vicinity of the wing dams. *n*=4 fish per class: fingerling, parr and adult. (A) Wavelength. (B) Tailbeat amplitude. (C) Tailbeat frequency. (D) Strouhal number (*St*). Swimming was in the freestream (blue) or vortex of a wing dam (red). Gray shading in D indicates the optimal range of *St* numbers (0.2–0.4; Taylor et al., 2003). Data are means±1 s.e.m.

classes, a smaller dam induced orientation more upstream, less time in the vortex, cross-stream position farther into the freestream flow and streamwise position further downstream (Fig. 4). This pattern of larger size classes being pushed further into the freestream flow suggests that a smaller size refuge was more difficult to refuge within, even for the fingerlings, though fingerlings were able to take advantage of the small vortices compared with parr and adults. Behavior behind the large dam suggests that all size classes preferred a vortex when they could take advantage of the low-speed, recurrent flow: all size classes spent more time within the vortex and tucked further away from freestream flow and further upstream against the dam.

Fish of all three size classes appeared to prefer microhabitat with low TKE. This is evident from comparing peak frequencies of position (Fig. 3) with TKE presented in Fig. 2C. TKE was greatest in the downstream portions of the shear layer (Fig. 2). TKE has been shown to increase swimming costs (Enders et al., 2005). Recent research shows that habitat with lower TKE assists migrating fish to pass pools or rest inside pools (Sirajee, 2023).

Implications for energetics of movement

The kinematics of trout swimming in the vortices of wing dams resembled the kinematics of Kármán gaiting and entrainment; they exhibited longer body wavelengths and lower tailbeat frequencies compared with freestream swimming (Liao et al., 2003a; Cook and Coughlin, 2010). One notable difference is that trout exhibited no significant difference in tailbeat amplitude between vortices and the freestream treatments, whereas tailbeat amplitude during Kármán gaiting and entrainment is greater than during freestream swimming (Liao et al., 2003a; Cook and Coughlin, 2010). Our results showing invariable amplitude across size reflect that tail movement will be influenced by the hydrodynamic patterns of flow during refuging downstream of the dam. Furthermore, the scaling of kinematic modulation within experimental flows differed between the two studies – smaller fish showed a longer body wavelength than larger fish when Kármán gaiting (Akanyeti and Liao, 2013), whereas scaling of wavelength increased with increasing size class in vortex swimming (Fig. 5). Our interpretation of these differences suggests

there are different kinematic solutions between energy harvesting and flow refuging. Kármán gaiting trout interacted with the outermost margin of vortices and adopted wavelengths to generally match the tangent of each vortex (i.e. not entering the vortex interior). In vortex refuging, the fish adopted kinematics to hold station within the vortex. This suggests the fish are conforming to the larger structure (as shown in the time-averaged wakes in Fig. 2) as opposed to the smaller vortex structures apparent in time-resolved samples (Fig. S1). Concurrent PIV and kinematics experiments would be necessary to resolve this.

Swimming kinematics in a vortex differed from that in freestream, falling outside the optimal *St* number range of $0.2 \leq St \leq 0.4$ for maximizing propulsive efficiency (Taylor et al., 2003; Fig. 5). This suggested that the fish did not seek to optimize undulatory kinematics when swimming in low-drag conditions. Drag is expected to vary with velocity squared. Average vortex velocity was ∼7.8 cm s^{-1}, 7.9 times less than average freestream velocity at ∼61.7 cm s^{-1}. Thus, we estimate drag for a given fish was ∼63 times less (i.e. 7.9^2=62.5) when swimming in vortices compared with the freestream. In contrast, in the freestream, parr and adults exhibited *St* numbers within the optimal range. Use of optimal *St* numbers in faster flow velocity is consistent with the hypothesis that efficient cruising is driven by drag (Floryan et al., 2018). We interpret that fingerlings lacked sufficient neuromuscular control, power or thrust production to achieve optimal *St* numbers in the freestream where average velocity (65 cm s^{-1}) was ∼12 BL s^{-1} for the fingerlings.

Two of our results are consistent with the hypothesis that fish find a behavioral solution to optimizing position within energetically favorable flows (Johansen et al., 2020). When dam size was adequate, fish chose to swim in the vortex, where flow velocity was ∼20% of freestream velocity, and in 17% of the experimental conditions fish swam on the inside edge of the shear layer (Figs 2, 3 and 4). Preferred swimming in low velocity flow is a feature of Kármán gaiting (Akanyeti and Liao, 2013). Alternative locations of swimming in the vicinity of obstacles include upstream in the bow wake and lateral entrainment (Liao et al., 2003b; Liao, 2007; Cook and Coughlin, 2010). Entrainment and Kármán gaiting are known to reduce metabolic costs as compared with swimming in the freestream (Cook and Coughlin, 2010), but energy savings are complicated by feeding (Johansen et al., 2020). Future research could combine detailed body kinematics with simultaneous time-resolved PIV to better inform bioenergetic models that can assess fish habitat quality and habitat restoration.

Conclusions

We observed significant effects of body size and dam size on swimming behavior and kinematics. Trout preferentially swam within the vortex of a wing dam when the relationship between vortex width and fish length (W_V:L_F) was >1.5. We estimate drag on the fish was 63 times lower in the vortex compared with the freestream, thus likely requiring much less energy for swimming. We interpret that smaller W_V:L_F ratios result in vortices that destabilize the fish. Our results may help inform ongoing efforts to improve existing stream habitat for trout (e.g. Shuler et al., 1994) and assist migrating fish to pass upstream of dams using vertical slot ladders (Forty et al., 2016; Hodge et al., 2017). Dam width may be a reasonable proxy for wake width for such field applications. Natural waterways are vastly more complex than our water flume (Fig. 1) and feature a diverse array of selective pressures (Rosenfeld and Boss, 2001) that may vary according to life history stage (Schluter et al., 1991). Thus, studies in natural streams are needed to further elucidate the ecological and evolutionary implications of our experiments.

Acknowledgements

We thank Anthony Lapsansky for participation in preliminary experiments and for our initial implementation of DeepLabCut, Dennin Holmes and Emma Musick for animal care, and Nick and Allen Harriman of Harriman Trout Company for supplying animals.

Competing interests

The authors declare no competing or financial interests.

Author contributions

Conceptualization: T.R.D., J.C.L., B.W.T.; Methodology: T.R.D., L.A.C., J.C.L., B.W.T.; Software: J.C.L., B.W.T.; Validation: J.C.L., B.W.T.; Formal analysis: T.R.D., J.C.L., B.W.T.; Investigation: T.R.D., L.A.C., J.C.L., B.W.T.; Resources: J.C.L., B.W.T.; Data curation: B.W.T.; Writing - original draft: T.R.D., B.W.T.; Writing - review & editing: T.R.D., J.C.L., B.W.T.; Visualization: B.W.T.; Supervision: J.C.L., B.W.T.; Project administration: L.A.C., J.C.L., B.W.T.; Funding acquisition: J.C.L., B.W.T.

Funding

The equipment and animal housing costs of this research were supported by funds from the Office of Naval Research (N000141912540), National Science Foundation (EFRI 1935216) and Drollinger Family Charitable Foundation to B.W.T. The study was supported by National Science Foundation (IOS 1856237 and PHY 2102891) and National Institutes of Health (R56DC020321) grants to J.C.L. Deposited in PMC for release after 12 months.

Data availability

The data that support the findings of this study are available from the Dryad Digital Repository (Dial et al., 2024): doi:10.5061/dryad.280gb5mzk.

References

Akanyeti, O. and Liao, J. C. (2013). The effect of flow speed and body size on Kármán gait kinematics in rainbow trout. *J. Exp. Biol.* **216**, 3442-3449. doi:10.1242/jeb.087502

Ayllón, D., Almodóvar, A., Nicola, G. G. and Elvira, B. (2010). Ontogenetic and spatial variations in brown trout habitat selection. *Ecol. Fresh. Fish.* **19**, 420-432. doi:10.1111/j.1600-0633.2010.00426.x

Baltz, D. M., Vondracek, B., Brown, L. R. and Moyle, P. B. (1991). Seasonal changes in microhabitat selection by rainbow trout in a small stream. *Trans. Am. Fish. Soc.* **120**, 166-176. doi:10.1577/1548-8659(1991)120<0166:SCIMSB>2.3.CO;2

Beal, D. N., Hover, F. S., Triantafyllou, M. S., Liao, J. C. and Lauder, G. V. (2006). Passive propulsion in vortex wakes. *J. Fluid Mech.* **549**, 385-402. doi:10.1017/S0022112005007925

Bouckaert, F. W. and Davis, A. J. (1998). Microflow regimes and the distribution of macroinvertebrates around stream boulders. *Freshw. Biol.* **40**, 77-86. doi:10.1046/j.1365-2427.1998.00329.x

Cook, C. L. and Coughlin, D. J. (2010). Rainbow trout Oncorhynchus mykiss consume less energy when swimming near obstructions. *J. Fish Biol.* **77**, 1716-1723. doi:10.1111/j.1095-8649.2010.02801.x

Cote, A. J. and Webb, P. W. (2015). Living in a turbulent world – a new conceptual framework for the interactions of fish and vortices. *Int. Comp. Biol* **55**, 662-672. doi:10.1093/icb/icv085

Currier, M., Rouse, J. and Coughlin, D. J. (2021). Group swimming behaviour and energetics in bluegill Lepomis macrochirus and rainbow trout Oncorhynchus mykiss. *J. Fish Biol.* **98**, 1105-1111. doi:10.1111/jfb.14641

Dial, T. R., Collins, L. A., Liao, J. C. and Tobalske, B. W. (2024). Body length determines flow refuging for rainbow trout (*Oncorhynchus mykiss*) behind wing dams. Dryad. doi:10.5061/dryad.280gb5mzk

Enders, E. C., Boisclair, D. and Roy, A. G. (2003). The effect of turbulence on the cost of swimming for juvenile Atlantic salmon (*Salmo salar*). *Can. J. Fish. Aquat. Sci.* **60**, 1149-1160. doi:10.1139/f03-101

Enders, E. C., Boisclair, D. and Roy, A. G. (2005). A model of total swimming costs in turbulent flow for juvenile Atlantic salmon (*Salmo salar*). *Can. J. Fish. Aquat. Sci.* **62**, 1079-1089. doi:10.1139/f05-007

Enders, E. C., Gessel, M. H. and Williams, J. G. (2009). Development of successful fish passage structures for downstream migrants requires knowledge of their behavioural response to accelerating flow. *Can. J. Fish. Aq. Sci.* **66**, 2109-2117. doi:10.1139/f09-141

Floryan, D., Van Buren, T. and Smits, A. J. (2018). Efficient cruising for swimming and flying animals is dictated by fluid drag. *Proc. Natl. Acad. Sci. USA* **115**, 8116-8118. doi:10.1073/pnas.1805941115

Forty, M., Spees, J. and Lucas, M. C. (2016). Not just for adults! Evaluating the performance of multiple fish passage designs at low-head barriers for the upstream movement of juvenile and adult trout *Salmo trutta*. *Ecol. Eng.* **94**, 214-224. doi:10.1016/j.ecoleng.2016.05.048

Gale, W. L., Hill, M. S. and Zydlewski, G. B. (2004). Physiological and behavioural differences of hatchery and wild–reared steelhead Oncorhynchus mykiss smolts

of the same genetic origin. *J. Fish Biol.* **65**, 328-329. doi:10.1111/j.1095-8649.2004.559ah.x

Hameed, I. H. and Hilo, A. N. (2021). Numerical analysis on the effect of slot width on the design of vertical slot fishways. *IOP Conf. Ser. Mater. Sci. Eng.* **1090**, 012094. doi:10.1088/1757-899X/1090/1/012094

Harvey, S. T., Muhawenimana, V., Müller, S., Wilson, C. A. and Denissenko, P. (2022). An inertial mechanism behind dynamic station holding by fish swinging in a vortex street. *Sci. Rep.* **12**, 12660. doi:10.1038/s41598-022-16181-8

Hedrick, T. L. (2008). Software techniques for two-and three-dimensional kinematic measurements of biological and biomimetic systems. *Bioinsp. Biomim.* **3**, 034001. doi:10.1088/1748-3182/3/3/034001

Hodge, B. W., Fetherman, E. R., Rogers, K. B. and Henderson, R. (2017). Effectiveness of a fishway for restoring passage of Colorado River cutthroat trout. *N. Am. J. Fish. Manage* **37**, 1332-1340. doi:10.1080/02755947.2017.1386144

Johansen, J. L., Akanyeti, O. and Liao, J. C. (2020). Oxygen consumption of drift-feeding rainbow trout: the energetic tradeoff between locomotion and feeding in flow. *J. Exp. Biol.* **223**, jeb220962. doi:10.1242/jeb.220962

Jonsson, N. and Jonsson, B. (1998). Body composition and energy allocation in life–history stages of brown trout. *J. Fish. Biol.* **53**, 1306-1316. doi:10.1006/jfbi.1998.0796

Kalb, B. W., Huntsman, B. M., Caldwell, C. A. and Bozek, M. A. (2018). A mechanistic assessment of seasonal microhabitat selection by drift-feeding rainbow trout Oncorhynchus mykiss in a Southwestern headwater stream. *Environmental Biology of Fishes* **101**, 257-273. doi:10.1007/s10641-017-0696-9

Kerr, J. R., Manes, C. and Kemp, P. S. (2016). Assessing hydrodynamic space use of brown trout, *Salmo trutta*, in a complex flow environment: a return to first principles. *J. Exp. Biol.* **219**, 3480-3491. doi:10.1242/jeb.134775

Liao, J. C. (2004). Neuromuscular control of trout swimming in a vortex street: implications for energy economy during the Karman gait. *J. Exp. Biol.* **207**, 3495-3506. doi:10.1242/jeb.01125

Liao, J. C. (2006). The role of the lateral line and vision on body kinematics and hydrodynamic preference of rainbow trout in turbulent flow. *J. Exp. Biol.* **209**, 4077-4090. doi:10.1242/jeb.02487

Liao, J. C. (2007). A review of fish swimming mechanics and behaviour in altered flows. *Philos. Trans. R. Soc. B Biol. Sci.* **362**, 1973-1993. doi:10.1098/rstb.2007.2082

Liao, J. C. and Cotel, A. (2013). Effects of turbulence on fish swimming in aquaculture. In *Swimming Physiology of Fish* (ed. A. P. Palstra and J. V. Planas). Springer.

Liao, J. C., Beal, D. N., Lauder, G. V. and Triantafyllou, M. S. (2003a). Fish exploiting vortices decrease muscle activity. *Science* **302**, 1566-1569. doi:10.1126/science.1088295

Liao, J. C., Beal, D. N., Lauder, G. V. and Triantafyllou, M. S. (2003b). The Kármán gait: novel body kinematics of rainbow trout swimming in a vortex street. *J. Exp. Biol.* **206**, 1059-1073. doi:10.1242/jeb.00209

Lohr, S. C. and West, J. L. (1992). Microhabitat selection by brook and rainbow trout in a southern Appalachian stream. *Trans. Am. Fish. Soc.* **121**, 729-736. doi:10.1577/1548-8659(1992)121<0729:MSBBAR>2.3.CO;2

Mathis, A., Mamidanna, P., Cury, K. M., Abe, T., Murthy, V. N., Mathis, M. W. and Bethge, M. (2018). DeepLabCut: markerless pose estimation of user-defined body parts with deep learning. *Nature Neuro* **21**, 1281-1289. doi:10.1038/s41593-018-0209-y

McPhee, M. V., Whited, D. C., Kuzishchin, K. V. and Stanford, J. A. (2014). The effects of riverine physical complexity on anadromy and genetic diversity in steelhead or rainbow trout *Oncorhynchus mykiss* around the Pacific Rim. *J. Fish. Biol.* **85**, 132-150. doi:10.1111/jfb.12286

Nath, T., Mathis, A., Chen, A. C., Patel, A., Bethge, M. and Mathis, M. W. (2019). Using DeepLabCut for 3D markerless pose estimation across species and behaviors. *Nature Prot.* **14**, 2152-2176. doi:10.1038/s41596-019-0176-0

Penaluna, B. E., Abadía-Cardoso, A., Dunham, J. B., García-Dé León, F. J., Gresswell, R. E., Luna, A. R., Taylor, E. B., Shepard, B. B., Al-Chokhachy, R., Muhlfeld, C. C. et al. (2016). Conservation of native Pacific trout diversity in western North America. *Fisheries* **41**, 286-300. doi:10.1080/03632415.2016.1175888

Penaluna, B. E., Dunham, J. B. and Andersen, H. V. (2021). Nowhere to hide: The importance of instream cover for stream–living coastal cutthroat trout during seasonal low flow. *Ecol. Freshw. Fish.* **30**, 256-269. doi:10.1111/eff.12581

Rosenfeld, J. (2003). Assessing the habitat requirements of stream fishes: an overview and evaluation of different approaches. *Trans. Am. Fish. Soc.* **132**, 953-968. doi:10.1577/t01-126

Rosenfeld, J. S. and Boss, S. (2001). Fitness consequences of habitat use for juvenile cutthroat trout: energetic costs and benefits in pools and riffles. *Can. J. Fish. Aquat. Sci.* **58**, 585-593. doi:10.1139/f01-019

Schluter, D., Price, T. D., Rowe, L. and Grant, P. R. (1991). Conflicting selection pressures and life history trade-offs. *Proc. R. Soc. Lond. B Biol. Sci.* **246**, 11-17. doi:10.1098/rspb.1991.0118

Shuler, S. W., Nehring, R. B. and Fausch, K. D. (1994). Diel habitat selection by brown trout in the Rio Grande River, Colorado, after placement of boulder structures. *N. Amer. J. Fish. Manage* **14**, 99-111. doi:10.1577/1548-8675(1994)014<0099:dhsbbt>2.3.co;2

Sirajee, M. N. (2023). An experimental study of fish movement with turbulent kinetic energy along the pools of a vertical slot fish pass. *Int. J. Env. Clim. Change* **13**, 2202-2215. doi:10.9734/ijecc/2023/v13i92454

Taguchi, M. and Liao, J. C. (2011). Rainbow trout consume less oxygen in turbulence: the energetics of swimming behaviors at different speeds. *J. Exp. Biol.* **214**, 1428-1436. doi:10.1242/jeb.052027

Taylor, G. K., Nudds, R. L. and Thomas, A. L. R. (2003). Flying and swimming animals cruise at a Strouhal number tuned for high power efficiency. *Nature* **425**, 707-711. doi:10.1038/nature02000

Tritico, H. M. and Cotel, A. J. (2010). The effects of turbulent eddies on the stability and critical swimming speed of creek chub (*Semotilus atromaculatus*). *J. Exp. Biol.* **213**, 2284-2293. doi:10.1242/jeb.041806

Werner, E. E. and Gilliam, J. F. (1984). The ontogenetic niche and species interactions in size-structured populations. *An. Rev. Ecol. System* **15**, 393-425. doi:10.1146/annurev.es.15.110184.002141

Williams, J. E., Williams, R. N., Thurow, R. F., Elwell, L., Philipp, D. P., Harris, F. A., Kershner, J. L., Martinez, P. J., Miller, D., Reeves, G. H. et al. (2011). Native fish conservation areas: a vision for large-scale conservation of native fish communities. *Fisheries* **36**, 267-277. doi:10.1080/03632415.2011.582398